Molecular Crystal Structure and Electron Density Distribution in the Crystal of Pentaethyl-1,5-dicarba-*closo*-pentaborane [C2B3(Et)5] at 120 K

Mikhael Antipin,*,† Roland Boese,*,§ Dieter Bläser,§ and Andreas Maulitz§

Contribution from the Institut für Anorganische Chemie, Universität-GH Essen, Universitätsstrasse 1-4, D-45117, Essen, Germany, and Institute of Organoelement Compounds, Russian Academy of Sciences (INEOS), Vavilov St. 28, B-334, Moscow, Russia

Abstract: The molecular and crystal structure and electron density distribution were studied for a single crystal of pentaethyl-1,5-dicarba-*closo*-pentaborane $C_2B_3(Et)_5$ by the high-resolution X-ray diffraction method at 120 K (5696 observed reflections, $R = 0.056$). The single crystal was grown by in situ crystallization with an IR-laser beam producing a molten zone in a Lindeman capillary. In crystal the molecule of the title compound has local C_1-symmetry with different orientations of the Et-groups with respect to the central trigonal-bipyramidal C_2B_3 fragment, mean B−C and B−B distances are 1.571 and 1.876 Å, respectively, the axial C...C distance is 2.277 Å. An *ab initio* calculations of the molecular structure indicated that rotation barriers of the Et groups with respect to the central frame are very small, that may be the reason of the low molecular symmetry and diffrerent orientation of the Et groups in molecule due to the crystal packing effects. Deformation electron density (DED) maps obtained via a conventional "X−X" method, and using a multipole refinement procedure, showed charge accumulation in the B−C bonds of the central frame, and these bonds were found to be essentially bent outward of the C_2B_3 cage. On the contrary, no charge accumulation was detected in the B−B bonds, thus indicating the absence of the direct B−B interactions. Positive and delocalized DED was also found in all B−C−B triangle faces of the central cage, that indicates the contribution of the multicenter bonding in the electronic structure of this formally electron-precise molecule. Topological analysis of the experimental charge density distribution has been performed including an analysis of the Laplacian maps, and these data confirmed all important features of the DED maps.

Introduction

X-ray structural studies of the polyhedral *closo*-borane dianions $B_nH_n^{2-}$, and isoelectronic *closo*-carboranes $C_2B_{n-2}H_n$ with $5 \leq n \leq 12$ having the closed deltahedral structures are rather scarce, with some exception for icosahedral boranes and carboranes ($n = 12$) and their numerous derivatives.[1] Understanding the molecular architecture and the nature of chemical bond in most of these compounds is possible in terms of the concept of the electron-deficite multicenter bonds.

Some concepts and electron counting rules were suggested in early days to describe the nonclassical structure of these molecules, starting from the first works by Longuet-Higgins[2,3] and Lipscomb.[4] Wade's rules[5,6] and Williams' classification[7] of *closo*-boranes and carboranes were found to be very useful in the assignment and prediction their molecular structures and relative stabilities of their isomers. More sophisticated models were developed and succesfully used later for describing the structure and bonding in this series of compounds, including Stone's surface harmonics approach,[8,9] graph-theoretical analysis,[10] and some others.[11,12]

The "six-electron rule" has been proposed by Jemmis[13] for explaining the stability of closed $B_nH_n^{2-}$ dianions and isoelectronic carboranes $C_2B_{n-2}H_n$. In accord with this rule the corresponding molecule or dianion, e.g. $B_nH_n^{2-}$, is considered as planar ring $(BH)_{n-2}$ with two caps $(BH)^-$ from both sides. Each boron atom of the ring forms three covalent bonds with the two neighboring boron and hydrogen atoms. A p orbital of each boron atom in the ring, directed along the normal to the ring plane, is empty. The $(BH)^-$ cap has five valence electrons, two of them are used to form the B−H bond, and three others are delocalized into the region of the cyclic $(n − 2)$ vacant p orbitals. Thus, two caps above and below the ring provide six valence electrons, and a relative stability of a given boran dianion or carborane molecule depends on the overlap between caps and ring orbitals. Caps with more diffuse orbitals prefer a larger rings and *vice versa* in order to maximize the orbital overlap. This "six-electron rule" was used often for explaining and predicting the molecular structures and relative stability of different heteroboranes including carboranes.

Nevertheless, none of the rules and concepts mentioned above can provide comprehensive knowledge about details of the electron density (or charge density) distribution (EDD) in these compounds, and in most cited papers such an analysis for polyhedral boranes and carboranes is missing. Meanwhile, EDD data should give direct information about the nature of the

† Institute of Organoelement Compounds, Russian Academy of Sciences.
§ University of Essen.
⊗ Abstract published in *Advance ACS Abstracts,* November 1, 1996.
(1) Beaudet, R. A. In *Advances in Boron and Boranes*; Liebmann, J. F., Greenberg A., Williams, R. E., Eds.; VCH Publishers: New York, 1988; Chapter 20, pp 417−429.
(2) Bell, R. P.; Longuet-Higgins, H. C. *Nature* **1945**, *155*, 328.
(3) Longuet-Higgins, H. C.; Phil, M. A. D. *Q. Rev. Chem. Soc.* **1957**, *11*, 121−133.
(4) Lipscomb, W. N. *Boron Hydrides*; Benjamin: New York, 1963.
(5) Wade, K. *J. Chem. Soc., Chem. Commun.* **1971**, 792−793.
(6) Wade, K. *Adv. Inorg. Radiochem.* **1976**, *18*, 1−66.
(7) Williams, R. E. *Chem. Rev.* **1992**, *92*, 177−207.

(8) Stone, A. J. *Mol. Phys.* **1980**, *41*, 1339−1354.
(9) Stone, A. J. *Inorg. Chem.* **1981**, *20*, 563−571.
(10) King, R. B.; Rouvray, D. H. *J. Am. Chem. Soc.* **1977**, *99*, 7834−7840.
(11) Gimarc, B. M. *J. Am. Chem. Soc.* **1983**, *105*, 1979−1984.
(12) King, R. B.; Dai, B.; Gimarc, B. M. *Inorg. Chim. Acta* **1990**, *167*, 213−222.
(13) Jemmis, E. D. *J. Am. Chem. Soc.* **1982**, *104*, 7017−7020.

chemical bond in terms of the topological properties and characteristics of the total electron density distribution function $\rho(r)$ of the molecular system including its gradient vector field $\nabla\rho(\mathbf{r})$, Laplacian, critical points, bond paths, etc.,[14,15] or in terms of the deformation (difference) electron density $\delta\rho(r)$, representing a difference between $\rho(r)$ and electron density of some specially defined reference state.[16] The values of $\rho(r)$ and $\delta\rho(r)$ may be reconstructed now with a high accuracy directly from X-ray diffraction data of single crystals,[16-18] or calculated by the modern methods of quantum chemistry. Comparison of these data has a great importance for understanding chemical bonding in different classes of compounds and for developing new models and concepts of the chemical bond, especially for the "nonclassical" compounds, where usual valence rules are not valid. However, for boranes and carboranes experimental X-ray diffraction studies of EDD are very rare, and only few compounds were studied recently, including the structure of the decaborane[19] and azido derivative of the icosahedral *m*-carborane.[20]

Ab initio quantum chemical calculations of boranes and carboranes were also a subject of few recent publications, but in most of these papers only the molecular geometries, relative stability of the possible isomers, or some special properties, i.e. [11]B chemical shifts, were investigated (see for example ref 21). During the last few years, only three papers were published[22-24] where an electronic structure of the *closo*-boranes and *closo*-carboranes was analyzed in the terms of EDD.

Takano et al.[22] have performed *ab initio* MO calculations for a series of *closo*-boranes $B_nH_n^{2-}$ and *closo*-carboranes $C_2B_{n-2}H_n$ ($5 \leq n \leq 12$) with deltahedral skeletons to study EDD features in the electron deficient three-center two-electron bonds. The deformation electron density maps in different sections were constructed for dianions $B_5H_5^{2-}$, $B_6H_6^{2-}$, and $B_7H_7^{2-}$, and it was established that the central planar ring has the same tendency for the charge distribution and stability as that in planar cyclic conjugated systems. The central part of the cages was found to be electronically empty and extra $(2-)$ charge in the dianions is delocalized on the surface of the cages.

In the paper of Bader and Legare[23] the molecular and electronic structures and properties of the 10 simplest boranes and carboranes were studied by *ab initio* SCF methods. The molecular structures were assigned on the basis of the bond paths (the lines of the maximum electron density linking atoms) defined by the topology of the charge density $\rho(r)$ using Bader's theory of atoms in molecules.[14] This theory was used to characterize the atomic interactions and to account for the

stability of these electron-deficient systems. The analysis of the critical points of the charge density and Laplacian distribution has shown that stabilization of these molecules is achieved not only by the electron density accumulation along the bond paths, but in addition by a concentration of electronic charge within, and its delocalization over the rings of bonded atoms, thus forming additional interatomic linkages. The lines of maximum electron density linking atoms in the three-membered rings in these electron deficient molecules have reduced bond orders in comparison with the formal two-electron bonds, but nevertheless a very pronounced degree of the electron delocalization of the minimum amount of the electron glue provides the maximum stability of these cage systems.

A very similar topographical analysis of the charge density distribution and molecular electroctatic potential was used by Jemmis et al.[24] in the theoretical study of the series of *n* vertex ($n = 5-7$) *closo*-boranes, -carboranes, and -silaboranes, and some conclusions about charge distribution and reactivity of these compounds were made.

In the papers[22-24] cited above, the structure of the 1,5-dicarba-*closo*-pentaborane, $C_2B_3H_5$ (**I**), having two carbon atoms in the apical positions of the trigonal bipyramid B_3C_2, was considered and discussed in detail. This molecule posseses two interesting features—in the series of all *closo*-carboranes, this is the smallest cage amongst the possible deltahedrons, and from the formal valence rules this is so-called electron-precise molecule, obeying the conventional description of the chemical bonding, if it is assumed *a priori* that there is no direct B—B bonding. Therefore, traditional schemes for small carboranes, i.e. the "six-electrons rule" by Jemmis,[13] probably should not work for description chemical bonds in **I**. On the other hand, the molecule **I** is isostructural and isoelectronic with the $B_5H_5^{2-}$ dianion, and the structure of this dianion is described usually in terms of the delocalized electron density.[22] It was noted earlier,[25] that the structure of the smallest *closo*-carboranes deserves special interest, since a multicenter bonding in these molecules at the faces of the cage is possible. Therefore we may expect that for molecule **I** and its derivatives the description of the bonding will be intermediate between the classical and nonclassical one.

An important result of the theoretical charge density studies of **I** was that this molecule does not exhibit any B—B bond paths in the equatorial plane, i.e. there are no direct B—B bonds, and axial B—C bonds are bent outward of the molecular cage.[23,24] In this respect $C_2B_3H_5$ differs essentially from the six-vertex and electron deficient $C_2B_4H_6$ and $B_6H_6^{2-}$ cages, where strong direct B—B bonds were found. There are also experimental electron diffraction data[26] for compound **I**, but these data cannot give information about charge density distribution and only proved the molecular structure and geometry. Therefore experimental EDD study of **I** or its derivatives by a high-resolution X-ray diffraction analysis of their single crystals seems to be very important for understanding the bonding situation in small carboranes.

In the present paper we report the results of the low temperature (120 K) X-ray diffraction study of the electron density distribution in the crystal of pentaethyl-1,5-dicarba-*closo*-pentaborane, $C_2B_3(Et)_5$ (**II**). This is the first experimental EDD study of the derivative of the smallest *closo*-carborane.

(14) Bader, R. F. W. *Atoms in Molecules: A Quantum Theory*; Oxford University Press: Oxford, U.K., 1990; 438 pp.

(15) Kraka, E.; Cremer, D. In *Theoretical Models of Chemical Bonding, Part 2. The Concept of the Chemical Bond*; Maksić, Z. B., Ed.; Springer-Verlag: Berlin-Heidelberg, 1990; pp 453–487.

(16) *The Applications of Charge Density Research to Chemistry and Drug Desigh;* Jeffrey, G. A., Piniella, J. F., Eds.; NATO ASI Series B, Vol. 250; Plenum Press: New York, 1991; 409 pp.

(17) Coppens, P. *Annu. Rev. Phys. Chem.* **1992**, *43*, 663–692.

(18) Hirshfeld, F. H. In *Accurate Molecular Structures.Their Determination and Importance*; Domenicano, A., Hargittai, I., Eds.; Oxford University Press: Oxford, U.K., 1992; Chapter 10, p 237.

(19) Dietrich, H.; Scheringer, C. *Acta Crystallogr., Ser. B* **1978**, *34*, 54–63.

(20) Antipin, M. Yu.; Poliakov, A. V.; Kapphan, M.; Tsirel'son, V. G.; Ozerov, R. P.; Struchkov, Y. T. *Organomet. Chem. USSR* **1990**, *3*, 421–426.

(21) Bühl, M.; Schleyer, P. v. R. *J. Am. Chem. Soc.* **1992**, *114*, 477–491.

(22) Takano, K.; Izuho, M.; Hosoya, H. *J. Phys. Chem.* **1992**, *96*, 6962–6969.

(23) Bader, R. F. W.; Legare, D. A. *Can. J. Chem.* **1992**, *70*, 657–676.

(24) Jemmis, E. D.; Subramanian, G.; Srivastava, I. H.; Gadre, R. *J. Phys. Chem.* **1994**, *98*, 6445–6451.

(25) Onak, T.; Fuller, K. In *Electron Deficient Boron and Carbon Clusters*; Olah, G. A., Wade, K., Williams, R. E., Eds.; Wiley: New York, 1991; p 183.

(26) McNeill, F. A.; Gallaher, K. L.; Scholer, F. R.; Bauer, S. H. *Inorg. Chem.* **1973**, *12*, 1208–2111.

Table 1. Crystal Data and Experimental Conditions for Structure Refinement

empirical formula	$C_{12}H_{25}B_3$
molecular weight, M	201.8
crystal system	monoclinic
space group	$P2_1/c$
a, Å	9.219(2)
b, Å	20.669(7)
c, Å	7.842(2)
β, deg	111.97(2)
V, Å^3	1385.8(8)
Z	4
ρ_c (g cm^{-3})	0.967
T (K)	120
radiation	Mo Kα
μ (mm^{-1})	0.050
$F(000)$	448
crystal size	cylinder diameter 0.3 mm
2θ range (deg)	3.0–90.0
scan type	Wyckoff
scan range (deg)	1.80 in ω
no. of reflns colld	8842
no. of unique reflns	6898
R_{merg}	0.033
no. of obsd reflns ($F \geq 4\sigma$)	5696
no. of params	237
R	0.056
Rw	0.075
goodness of fit	1.18
weight scheme	$w^{-1} = \sigma^2(F) + 0.0021F^2$
largest differencepeak/hole (e/Å^3)	0.31/−0.21

The new route to the synthesis of **II** and some characteristics of its molecular structure were shortly described in ref 27.

Experimental Section and Structure Refinement

The title compound (**II**) at ordinary conditions represents a low melting colourless liquid with mp 211.5 K (see ref 28). The single crystal was grown at 193 K by an in situ crystallization technique using a miniature zone-melting method with the IR-laser beam producing a molten zone in a Lindeman capillary.[29] X-Ray diffraction data were obtained with a Siemens R3m/V diffractometer (graphite monochromator, Mo Kα radiation) at the temperature 120 K. The duration of the data collection period was about 130 h. The experimental and conventional refinement data are presented in Table 1. All intensities were corrected for the cylindrical shape of the crystal and absorption. The structure was solved and refined with the direct methods and full-matrix least-squares procedure in the anisotropic−isotropic (hydrogen atoms) approximation using the SHELXTL PLUS program package, including the isotropic extinction correction. The atomic coordinates and anisotropic displacement parameters for non-hydrogen atoms and hydrogen atoms coordinates with their isotropic displacement parameters are given in the Supporting Information.

In order to visualize the charge redistribution due to the chemical bond formation the deformation electron density (DED) maps were calculated for different sections of **II** using the standard "X−X" method.[16−18] These maps show the migration of the electron density with respect to the hypothetical superposition of the spherically averaged atomic densities centered at the real atomic positions in the crystal ("promolecule"). Atomic coordinates and anisotropic displacement parameters of the non-hydrogen atoms for the promolecule were refined using a high-order refinement of the diffraction data (3200 independent reflections with sin $\theta/\lambda \geq 0.60$ Å^{-1} and $|F| \geq 6\sigma(F)$, $R = 0.053$, Rw $= 0.067$, GOF $= 0.95$). H-Atom positions in this refinement were fixed at ideal distances of 1.08 Å together with their isotropic

(27) Köster, R.; Boese, R.; Wrackmeyer, B.; Schlanz, H.-J. *J. Chem. Soc., Chem. Commun.* **1995**, 1691−1692.

(28) Köster, R.; Horstschäfer, H.-J.; Binger, P.; Mattschei, P. K. *Liebigs Ann. Chem.* **1975**, 1339−1343.

(29) Boese, R.; Nussbaumer, M. In *Correlations, Transformations, and Interactions in Organic Crystal Chemistry, IUcr Crystallographic Symposia*; Jones, D. W., Katrusiak, A., Eds.; Oxford University Press: Oxford, U.K., 1994; Vol. 7, p 20.
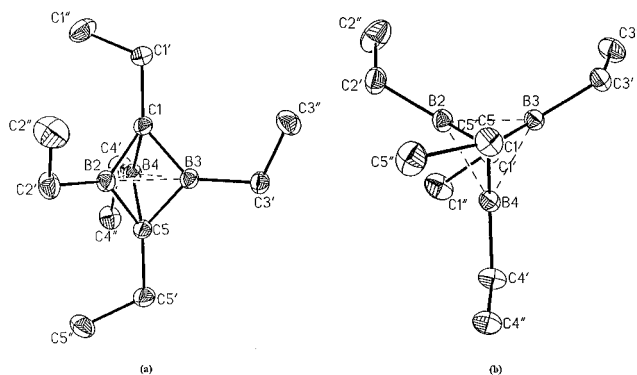
Figure 1. General view of the molecular structure of **II** in two projections and atom numbering scheme: (a) "side on" view; (b) view from the "top".

displacement parameters. In the subsequent Fourier-calculations of the DED maps only the low-angle data with sin $\theta/\lambda \leq 0.70$ Å^{-1} and $|F| \geq 4\sigma(F)$ were used in order to decrease the noise due to the relative inaccuracy of the high-angle data.

A multipole refinement of the X-ray diffraction data using a model of the rigid nonspherical pseudoatom by Hansen and Coppens[30] has been carried out in order to get so-called "static" DED maps and calculate some properties and characteristics of the total electron density $\rho(r)$, including its Laplacian $-\nabla^2\rho(r)$ and bond critical points in $\rho(r)$. The nonspherical atom model of Hansen and Coppens is commonly used to present the atomic charge density distribution in the analytical form as the sum of the three components:

$$\rho(\mathbf{r}) = P_c\rho_c(r) + P_v k'^3 \rho_v(k'r) + \rho_d(k''r)$$

where $\rho_c(r)$ and $\rho_v(r)$ are the spherically averaged Hartree−Fock atomic core and valence densities, respectively, and the term $\rho_d(r)$ describes the valence shell deformations as a series expansion with the Slater-type radial functions $R_l(k''r)$ modulated by the normalized angular harmonic functions d_{lmp} (multipoles) up to order of 4, and related to the real spherical harmonics y_{lmp}, which describe the angular part of the hydrogenic wavefunctions. Thus, the term $\rho_d(k''r)$ describing the electron density deformations may be written as

$$\rho_d(k''r) = \sum_{l=o}^{l_{max}} k''^3 R_l(k''r) \sum_{m=o}^{l} \sum_{p} P_{lmp} d_{lmp}(\mathbf{r}/r)$$

where P_c, P_v, and P_{lmp} are the population coefficients, p can be + or − for non-zero l, and k' and k'' are the values describing the contraction (expantion) of the atomic valence shells. All these values are refined by the least-squares together with the atomic coordinates and displacement parameters using diffraction data. More detailed description of this multipole model is given elsewhere.[16−18,30]

In this paper we used the new XD program package[31] for multipole charge density analysis in the structure of **II**. To reduce the number of refined parameters a local symmetry and "chemical" constrains were imposed on the multipole coefficients. Thus, all chemically equivalent atoms in the molecule were assumed to have the same deformation, and for C(1), C(1′), C(1″), C(2′), C(2″), and B(2) atoms (see Figure 1), the local symmetry was considered to be 3m, m, 3m, m, 3m, and mm2, respectively. This allowed a reduction of the number of refined multipole parameters P_v and P_{lmp} to the value of 59 with the multipole expansion to the hexadecapole level ($l = 4$) for B and C atoms, and dipole level ($l = 1$) for H atoms. This refinement converged to $R = 0.044$ and Rw $= 0.041$, which was a significant improvement in comparison with the conventional one (Table 1). The relatively high R values in all refinements probably are due to a nonsufficient accuracy of the high-order diffraction data. The release of the local symmetry

(30) Hansen, N. K.; Coppens, P. *Acta Crystallogr., Ser. A* **1978**, *34*, 909−921.

(31) Koritsanszky, T.; Howard, S.; Mallinson, P. R.; Su, Z.; Richter, T.; Hansen, N. K. *XD−Computer Program Package for Multipole Refinement and Analysis of Electron Densities from Diffraction Data*, Version 1995.

Table 2.

Bond Lengths (Å)			
C(1)−C(1′)	1.508(1)	C(1)−B(2)	1.577(1)
C(1)−B(3)	1.561(1)	C(1)−B(4)	1.573(1)
C(1′)−C(1″)	1.526(1)	B(2)−C(2′)	1.580(2)
B(2)−B(3)	1.873(1)	B(2)−B(4)	1.882(2)
B(2)−C(5)	1.571(1)	C(2′)−C(2″)	1.521(2)
B(3)−C(3′)	1.575(1)	B(3)−B(4)	1.872(1)
B(3)−C(5)	1.574(1)	C(3′)−C(3″)	1.535(1)
B(4)−C(4′)	1.575(2)	B(4)−C(5)	1.567(1)
C(4′)−C(4″)	1.528(1)	C(5)−C(5′)	1.508(1)
C(5′)−C(5″)	1.534(1)		

Bond Angles (deg)			
C(1′)−C(1)−B(2)	136.5(1)	C(1′)−C(1)−B(3)	137.8(1)
B(2)−C(1)−B(3)	73.3(1)	C(1′)−C(1)−B(4)	134.8(1)
B(2)−C(1)−B(4)	73.4(1)	B(3)−C(1)−B(4)	73.3(1)
C(1)−C(1′)−C(1″)	112.8(1)	C(1)−B(2)−C(2′)	133.2(1)
C(1)−B(2)−B(3)	53.0(1)	C(2′)−B(2)−B(3)	149.1(1)
C(1)−B(2)−B(4)	53.2(1)	C(2′)−B(2)−B(4)	151.1(1)
B(3)−B(2)−B(4)	59.8(1)	C(1)−B(2)−C(5)	92.6(1)
C(2′)−B(2)−C(5)	134.2(1)	B(3)−B(2)−C(5)	53.5(1)
B(4)−B(2)−C(5)	53.1(1)	B(2)−C(2′)−C(2″)	113.9(1)
C(1)−B(3)−B(2)	53.7(1)	C(1)−B(3)−C(3′)	134.9(1)
B(2)−B(3)−C(3′)	149.5(10	C(1)−B(3)−B(4)	53.6(1)
B(2)−B(3)−B(4)	60.3(1)	C(3′)−B(3)−B(4)	150.1(1)
C(1)−B(3)−C(5)	93.0(1)	B(2)−B(3)−C(5)	53.4(1)
C(3′)−B(3)−C(5)	132.1(1)	B(4)−B(3)−C(5)	53.2(1)
B(3)−C(3′)−C(3″)	115.0(1)	C(1)−B(4)−B(2)	53.4(1)
C(1)−B(4)−B(3)	53.0(1)	B(2)−B(4)−B(3)	59.9(1)
C(1)−B(4)−C(4′)	131.9(1)	B(2)−B(4)−C(4′)	151.0(1)
B(3)−B(4)−C(4′)	149.0(1)	C(1)−B(4)−C(5)	92.8(1)
B(2)−B(4)−C(5)	53.2(1)	B(3)−B(4)−C(5)	53.6(1)
C(4′)−B(4)−C(5)	135.3(1)	B(4)−C(4′)−C(4″)	116.5(1)
B(2)−C(5)−B(3)	73.1(1)	B(2)−C(5)−B(4)	73.7(1)
B(3)−C(5)−B(4)	73.2(1)	B(2)−C(5)−C(5′)	136.2(1)
B(3)−C(5)−C(5′)	134.8(1)	B(4)−C(5)−C(5′)	138.2(1)
C(5)−C(5′)−C(5″)	113.4(1)		

and chemical constrains (boron and carbon atoms of the B_3C_2 central fragment were still chemically constrained) resulted to the lower *R* values ($R = 0.039$, *R*w $= 0.036$), but the esd's in the refined parameters were larger than in the constrained refinement, and some of the multipole parameters had nonreasonable values. But, the main characteristics of the calculated DED maps were very similar for both refinements and very close to those obtained by the "X−X" method, therefore further only the data of the constrained refinement will be discussed.

Results and Discussion

Molecular Structure. The general view of the molecular structure of (**II**) in two projections "side on" and from the "top" is shown in Figure 1, the bond lengths and bond angles are presented in Table 2. In the crystal the molecule has local C_1 symmetry in contrast to the nonsubstituted *closo*-$C_2B_3H_5$ (**I**) with D_{3h} symmetry in the gas phase in accord with the electron diffraction data.[26] The low molecular symmetry of **II** in the crystal is related with the nonregular orientation of Et groups at the boron atoms with respect to the equatorial B_3-plane (see Figure 1). Thus, the torsion angles C(2″)C(2′)B(2)C(1), C(3″)C(3′)B(3)C(1), and C(4′)C(4′)B(4)C(1) characterizing the orientation of these groups, are −34.4, 17.4, and −176.4°, respectively. This difference may be a result of crystal packing requirements (see below).

The geometrical parameters of the molecular structure of **II** have expected values. In the central C_2B_3 fragment the mean B−B (1.876(4) Å) and B−C (1.571(5) Å) bond lengths are longer than corresponding values for **I** in the gas phase (1.853-(2) and 1.571(5) Å). This gives a longer C(1)⋯C(5) distance in **II** in comparison with **I**−2.277(1) and 2.261(3) Å. The endocyclic bond angles B−C−B (73.05(1) and 73.3(3)° for **I**

and **II**, respectively), and C−B−C (93.16(1) and 92.8(2)°) in both molecules are very similar, probably indicating the rigidity of the cage structure. It is interesting to note that the mean B−C(1,5) distance 1.571(5) Å in the cage is almost the same as the mean B−C(Et) bond length 1.577(2) Å, and these values are close to the mean B−C bond length in the structure of triethylborane (1.573(1) Å in accord with the X-ray data[32]).

The molecule **II** is electron precise, therefore its structure may be described without suggesting the existence of direct B−B bonds, although the B−B distances are rather short. Thus, the coordination of the boron atoms may be considered as formally trigonal, and these atoms should belong to the planes of their neighbouring carbon atoms forming planar C_3B fragments. These fragments were found to be strictly planar, the mean-squared deviation of the atoms from the corresponding planes are less than 0.005 Å. The empty p orbitals of the boron atoms in this case should be directed perpendicular to these C_3B planes, i.e. they should be positioned in the equatorial B−B−B plane of the molecule.

This description allows an explanation for the observed differences in the C−C−B bond angles in Et groups at the boron atoms by hyperconjugation effects.[32,33] Thus, the C−C−B bond angles at C(2′), C(3′), and C(4′) atoms are significantly different (113.9(1), 115.0(1), and 116.5(1)°, respectively), and this increasing of the angles correlates well with the corresponding torsion angles C−C−B−C(1). The more the Et groups are perpendicular to the B−B−B plane, the larger are corresponding C−C−B bond angles, and *vice versa* (the interplanar angles C−C−B/B−B−B for Et groups at B(2), B(3), and B(4) atoms are 54.3, 72.3, and 85.0°). It was shown that similar effects are caused by hyperconjugation, that influences the ZCC bond angles in main element (Z) ethyl compounds.[32] Thus, for a boryl group (Z = −BH_2) in accord with the MP2/6-31G* calculation the ZCC angle is equal to 105.3° if the empty p orbital of the boron lies in the C−C−B plane, because this conformation is favorable for hyperconjugation. If the empty p orbital of the B-atom is perpendicular to the C−C−B plane, the C−C−B angle is influenced indirectly, first via decreasing the H−C−H bond angle (electrons are withdrawn from CH_2 orbital with π-symmetry), and increasing the C−C−B bond angle as a consequence. For this conformation of $B(Et)_3$ the calculation (MP2/6-31G*) gives the value of the C-C-B angle 117.4°, that is close to the X-ray data (118.4°). The manifestation of this effect and its influence on the conformations of symmetric triethyl derivatives of boroxin, borazine, benzene, and triazine was also discussed.[33]

In order to establish the most important reason for the different orientation of Et groups, quantum chemical calculations of **II** were carried out using the SPARTAN 4.0 program package.[34] Five different conformations were considered as starting ones for the *ab initio* HF/3-21G geometry optimizations. In four conformations, two B-ethyl groups were pointed to one side of the B−B−B plane and the third B-ethyl group was pointed to the other side, the difference was in the orientation of the C-ethyl groups. In the fifth conformation the three B-ethyl groups were in the B−B−B plane. All optimizations allowed any orientation of the Et groups (C_1 symmetry). The total energy differences of the optimized structures were in the range of 0.7 kcal/mol, that is quite small. To get further insight

(32) Boese, R.; Bläser, D.; Niederprüm, N.; Nüsse, M.; Brett, A.; Schleyer, P. v. R.; Bühl, M.; Nicolaas, J. R.; Hommes, E. *Angew. Chem., Int. Ed. Engl.* **1992**, *31*, 314−316.

(33) Maulitz, A. H.; Stellberg, P.; Boese, R. *J. Mol. Struct. (THEOCHEM)* **1995**, *338*, 131−140.

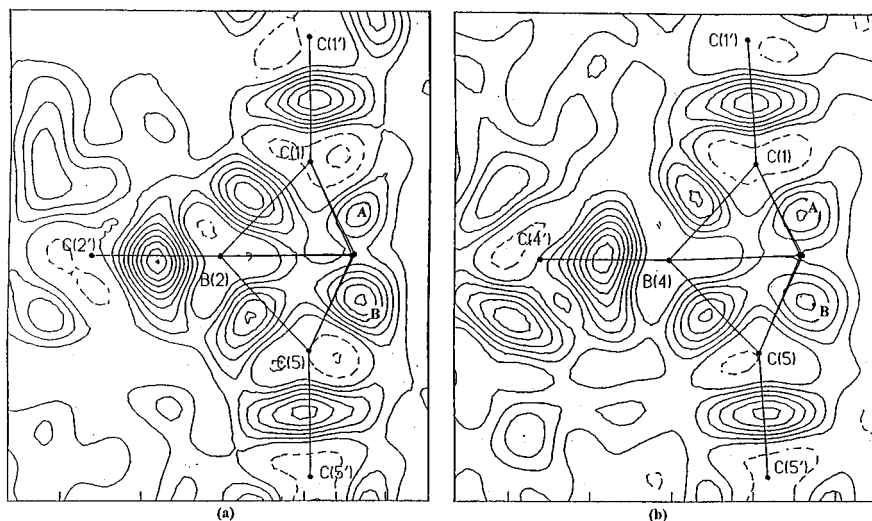(34) SPARTAN version 4.0, Wavefunction Inc., 18401 Von Karman Ave., N 370, Irvine, CA 92715.

Figure 2. DED maps ("X−X" method) in the axial planes of the central C_2B_3 fragment: (a) Section through atoms C(2′), B(2), C(1), C(5). (b) Section through atoms C(4′), B(4), C(1),C(5). Atoms C(1′) and C(5′) belong to the same planes. In all figures with DED maps contours between isolines are −0.1 and 0.05 e/Å^3, negative contours dashed.

in the preferred orientation of the Et groups with respect to the B_3C_2 frame, an optimization of both B-monoethyl (a) and C-monoethyl (b) derivatives of the $C_2B_3H_5$ structure was carried out in the HF/6-31G(d) approximation. In the optimized structures the orientation of the C-ethyl group was found to be in agreement with the experimental data, whereas the experimental orientation of only one of the B-ethyl groups was similar to the *ab initio* structure. The rotation barriers of the Et groups with respect to the central frame were found to be 0.6 and 0.8 kcal/mol, respectively for (a) and (b), indicating probably that orientation of all Et groups in the crystal structure of **II** might be determined by the crystal packing effects.

Charge Density Analysis. The deformation electron density maps obtained by the "X−X" method in two sections of (**II**) through apical C(1) and C(5) atoms and boron atoms B(2) and B(4) are presented in Figure 2a,b. These planes cut also the centre of the trigonal bipyramid C_2B_3 and the middles of the B(3)−B(4) and B(2)−B(3) bonds. Positive DED peaks with the heights 0.25−0.45 e/Å^3 were found nearly in the middles of all B−C bonds in these maps, thus indicating that these bonds are probably localized. Two interesting features of the maps presented should be noted. First, there are significant shifts of the DED maxima from the centers of B−C(1,5) bonds outward of the C_2B_3 cage, indicating the bending of these bonds. The values of shifts are 0.18−0.26 Å, that is comparable with the same shifts in small strained molecules like cyclopropane and annulated with benzene and naphtalene derivatives of cyclopropene (see, for example, refs 35 and 36). Another important feature of the maps discussed is the presence of the positive DED peaks not only in the B−C bonds (localized bonds), but also near the middles of the B−C−B triangles. These maxima (indicated as A and B in Figure 2a,b) have smaller heights (0.15−0.30 e/Å^3) than those in the B−C bonds, and they are localized a little above the B−C−B planes. The presence of these DED peaks may be considered as an indication of the multicenter bonding at the faces of the cage, that gives an additional contribution to the electronic structure of **II**.

Thus, DED maps clearly show that the bonding in the molecule **II** has in part multicenter character. It is interesting to note that similar DED section in $B_5H_5{}^{2-}$ dianion (*ab initio* calculation[22]), isoelectronic with $C_2B_3H_5$, is characterized by

almost the same features, namely by the bent B−B bonds and multicenter bonding in the B−B−B triangle faces. Moreover, DED section through the center of the tetrahedron cage in the structure of tetra-*tert*-butyltetrahedrane[37] is very close to that presented in Figure 2. We may conclude therefore that in small B,C cages characterized by the small endocyclic bond angles at boron and carbon atoms, there must be a multicenter bonding at the faces of the cages, whether a molecule is electron precise or not.

Some other DED sections in the molecule **II** are presented in Figure 3, namely sections containing triangle faces B(2)−C(1)−B(3) and B(2)−C(1)−B(4) (Figure 3a,b), and sections in the plane parallel to the B(2)−B(3)−B(4) plane, but shifted by 0.60 Å to the C(1) atom (Figure 3c). The last section cuts nearly the DED maxima in the axial B−C bonds and maxima A shown in Figure 2. These maps allow to estimate the relative contribution of the classical and nonclassical multicenter bonding. Thus, sections in Figure 3a,b in addition to the positive DED peaks in the B−C lines are characterized also by an essential delocalization of the positive DED in the triangle faces, and a section in Figure 3c has almost ringlike character. It is evident therefore, that for the molecule studied the contribution of the multicenter bonding may have almost the same importance as the classical one, although it is difficult to give some definite quantitative evaluation of these two contributions in terms of the DED analysis. Nevertheless, we can estimate from the heights of the DED maxima that the multicenter bond electron density is at least one-half of that for classical B−C bond.

DED section in the plane of the three boron atoms is presented in Figure 4. It is characterized by the absence of significant DED peaks in the B−B bonds, indicating that there is no direct B−B bonding in the molecule. This section is also very similar to that for $B_5H_5{}^{2-}$ dianion,[22] and agrees well with the data[23,24] for $C_2B_3H_5$, where the absence of the bond path (covalent bond) between boron atoms was established.

The static DED maps obtained via multipole refinement for sections in the axial C(1)−B(2)−C(5) and equatorial B(2)−B(3)−B(4) planes are shown in Figures 5 and 6. The DED features discussed above for dynamic "X−X" maps (Figures 2−4) were reproduced in the corresponding static maps in all

(35) Nijveldt, D.; Vos, A. *Acta Crystallogr., Ser. B* **1988**, *44*, 129.

(36) Boese, R. In *Advances in Strain in Organic Chemistry;* Halton, B., Ed.; J.A.I. Press: New York, 1992; Vol. 2, p 191.

(37) Irngartinger, H.; Jahn, R.; Maier, G.; Emrich, R. *Angew. Chem., Int. Ed. Engl.* **1987**, *26*, 356−357.
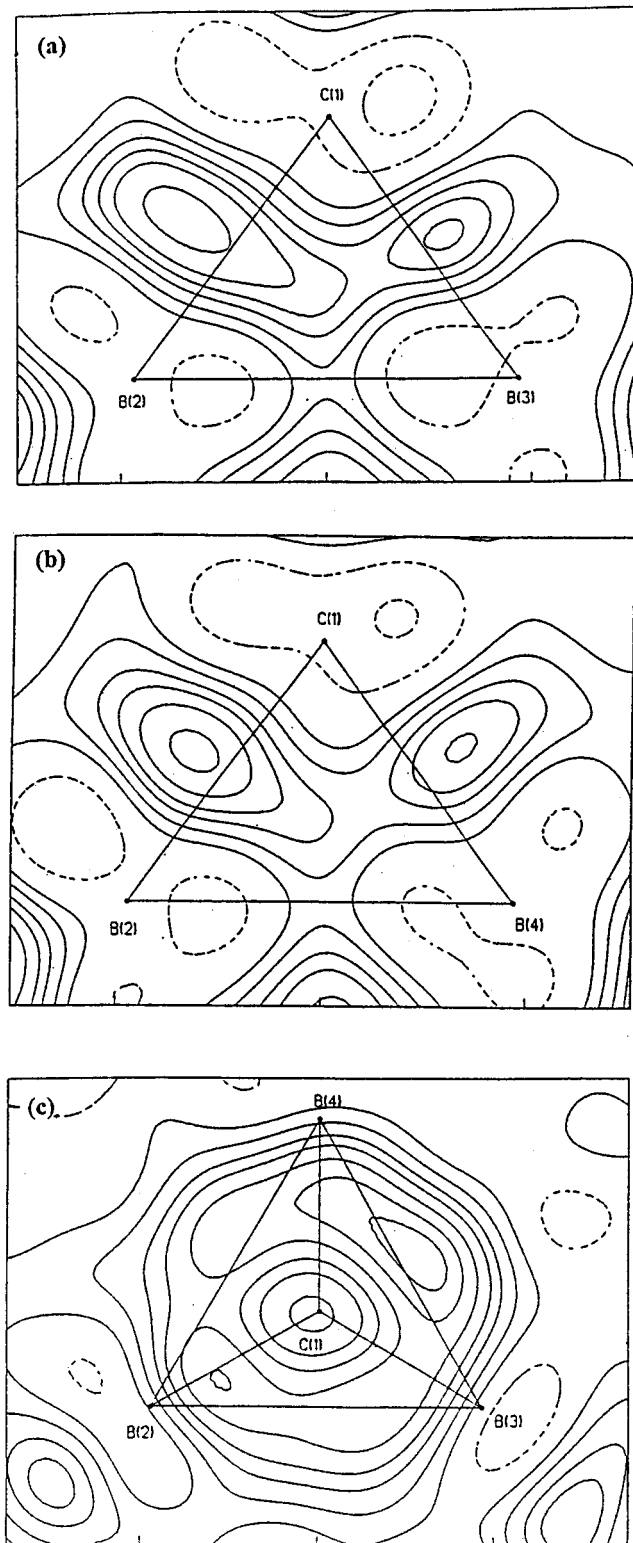
Figure 4. DED map ("X−X" method) in the equatorial B−B−B plane. Atoms C(2′), C(3′), and C(4′) are in the same plane.

Figure 3. DED maps ("X−X" method) in the triangle faces C(1)B-(2)B(3) and C(1)B(2)B(4) of the central cage (Figure 3a,b) and in the plane parallel to the B−B−B plane and shifted by 0.60 Å to the C(1) atom (Figure 3c).

important details, including the bending of the B−C bonds, multicenter bonding in the B−C−B faces, and the absence of the direct B−B bonds. Again we may note almost the total coincidence the maps in Figures 5 and 6 with the corresponding maps for $B_5H_5^{2-}$ dianion.

An important advantage of the multipole model is an opportunity to present the total electron density $\rho(r)$ in the analytical form. Therefore many one-electron properties of
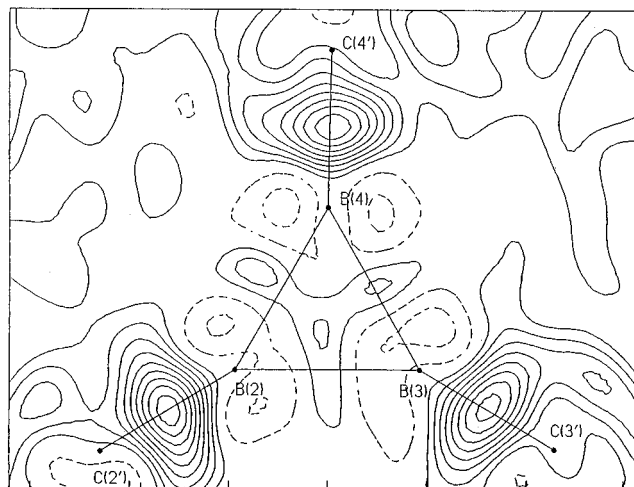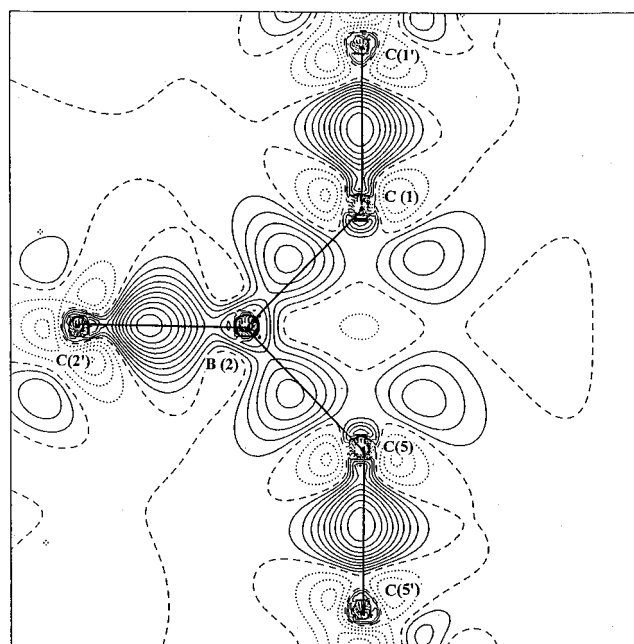

Figure 5. Multipole static DED map in the axial C(1)B(2)C(5) plane (the same section as in Figure 2).

molecules and crystals may be calculated now directly from the X-ray diffraction data.[16−18,38,39] Moreover, detailed analysis of the topological characteristics of the experimentally reconstructed function $\rho(r)$, including its Laplacian, types and positions of the critical points, bond path determination, etc., may be fulfilled following the Bader's theory of atoms in molecules.[14] In the present paper we performed such kind of analysis of the charge distribution in molecule **II** using XD package program.[31] It should be mentioned that in literature there are only few examples of the similar approach in the $\rho(r)$ analysis based on the experimental X-ray diffraction data, and this analysis has been done only for small organic molecules.[39−42]

Important topological properties of a scalar function such as $\rho(r)$, or its Laplacian $\nabla^2\rho(r)$, are summarized in terms of their

(38) Zu, Z.; Coppens, P. *Acta Crystalloogr., Ser. A* **1992**, *48*, 188−197.
(39) Howard, S. T.; Hursthouse, M. B.; Lehmann, C. W. *Acta Crystallogr., Ser. B* **1995**, *51*, 328−337.
(40) Gatti, C.; Bianchi, R.; Destro, R.; Merati, F. *J. Mol. Struct. (THEOCHEM)* **1992**, *255*, 409−433.
(41) Stewart, R. F. In *The Application of Charge Density Research to Chemistry and Drug Design*; Jeffrey, J. A., Piniella, J. F., Eds.; NATO ASI Series B, Vol. 250; Plenum Press: New York, 1991; p 63−101.
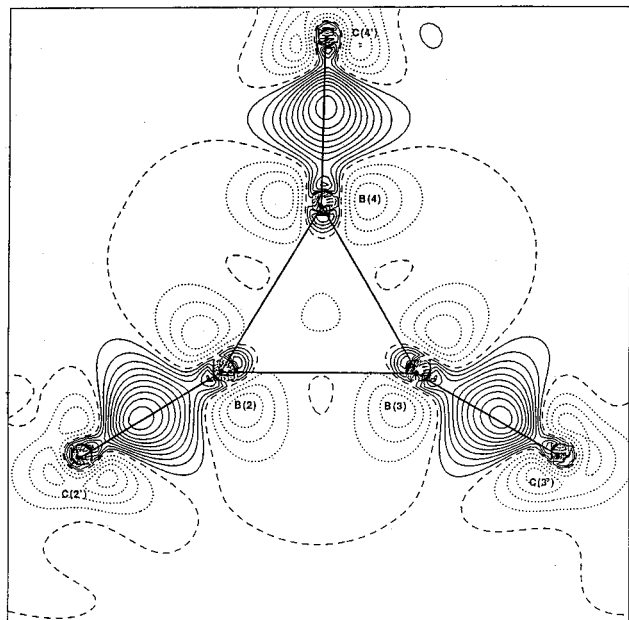
Figure 6. Multipole static DED map in the B−B−B plane (the same section as in Figure 4).

Figure 7. The map of the Laplacian of the $\rho(r)$ (as sections of the $-\nabla^2\rho(r)$ function) in axial plane of the molecule **II**.

critical points r_c. According to ref 14 only four types of the critical points of $\rho(r)$ are possible in a molecular system, namely $(3,-3)$, $(3,+3)$, $(3,+1)$, and $(3,-1)$ points. The $(3,-3)$ critical points correspond to the local maxima in $\rho(r)$ at the positions of atomic nuclei. The positions of the local minima of $\rho(r)$ are determined by the $(3,+3)$ critical points, and these points define the molecular cages and should be found incside them including cagelike structures of the *closo*-boranes and *closo*-carboranes. The special $(3,+1)$ critical points define the ring (cycle) structures. The more important are $(3,-1)$ critical points—the saddle points of $\rho(r)$ between the bonded atoms. The presence of this point between two atoms is considered as a necessary criteria of the covalent bond.[15]

The values of $\rho(r)$ and $\nabla^2\rho(r)$ in the $(3,-1)$ critical point, define many properties of the chemical bond. It was established for example for a series of organic molecules that the values of $\rho(r)$ in these points correlate with the corresponding bond lengths and bond orders.[15,43] Two negative curvatures of $\rho(r)$ define an ellipticity of the bond which is a measure of the charge accumulation in a given plane. The sum of three curvatures equals the Laplacian of $\rho(r)$, and negative values of $\nabla^2\rho(r)$ indicate those regions of the molecular space where a local charge concentration takes place. It is important that Laplacian is calculated directly from $\rho(r)$ and it is not a model-dependent difference function as does DED. Therefore an analysis of the Laplacian maps gives an additional independent information about EDD characteristics and the chemical bonding.

Experimental Laplacian map (as sections of the $-\nabla^2\rho(r)$ function) in the axial plane of the C_2B_3 fragment of **II** is presented in Figure 7, and a three-dimensional plot of the same function in the B−B−B plane is shown in Figure 8.

The general view of these maps confirms main conclusions about chemical bonding in **II** based on the analysis of dynamic ("X−X") and static (multipole) DED maps. Thus, in Figure 7 the regions of the negative Laplacian are concentrated almost at the same positions as do positive maxima in the DED maps. The above-mentioned bond bending in the axial B−C bonds is clearly seen in Figure 7, as well as charge accumulation (maxima
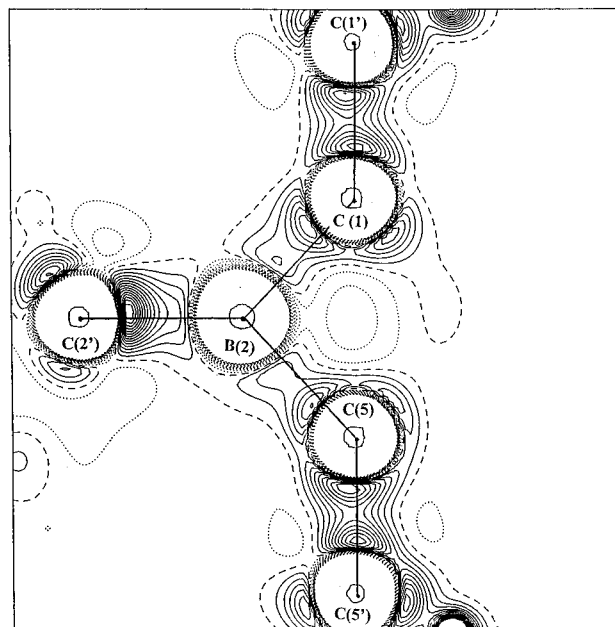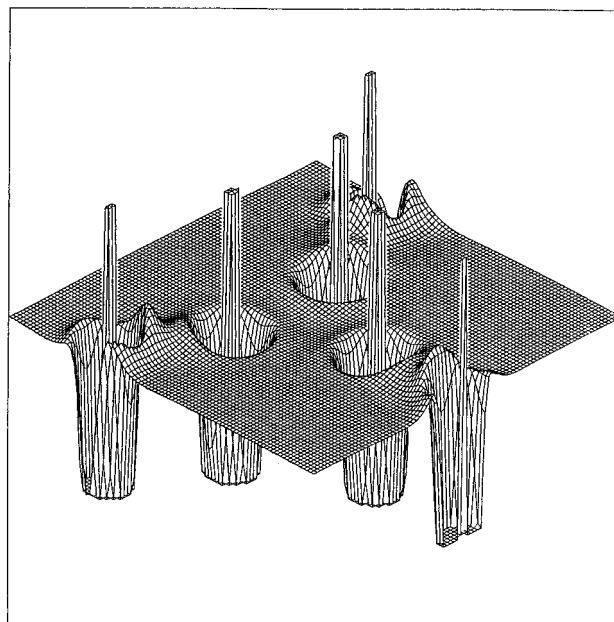

Figure 8. Three-Dimensional plot of the Laplacian $(-\nabla^2\rho(r))$ electron density in the plane of the boron atoms.

of the $-\nabla^2\rho(r)$, respectively) in the triangle B−C−B faces of the C_2B_3 cage (compare Figures 2, 5, and 7). The central of the cage is characterized by the positive values of Laplacian indicating charge depletion in this region. This may be seen also in Figure 8, where the B−B−B section of the negative Laplacian has an almost flat relief in the region of the B−B bonds (no bonds between these atoms), slight negative values in the center of the cage (minimum of the charge density), and well defined maxima of $-\nabla^2\rho(r)$ in the covalent B−C(Et) bonds.

Some topological characteristics of the charge density in molecule **II** are presented in Table 3, where similar values (if calculated by an *ab initio* in refs 23, 24) for the $C_2B_3H_5$ molecule **I** are also given for comparison.

Presented data show that axial B−C bonds in both molecules are characterized by the $(3,-1)$ bond critical points, whereas near the B−B lines there are only "ring" $(3,+1)$ critical points, and the centre of the cages is characterized by a $(3,+3)$ critical

(42) Destro, R.; Merati, F. *Acta Crystallogr., Ser. B* **1995**, *51*, 559−570.

(43) Cremer, D.; Kraka, E. *Croat. Chem. Acta* **1984**, *56*, 1259.

Table 3. Some Topological Characteristics of the Charge Density Distribution $\rho(r)$ in the C_2B_3 Cages of Molecules **I** and **II**

characteristic	B–C bond	B–B bond	center of the cage
type of critical point	(3,−1)	(3,+1)	(3,+3)
R (Å)[a]	1.554	1.885	
	1.560		
	1.571	1.876	
ρ_c (e/Å^3)	1.142	0.682	0.615
	1.138	–	0.613
	1.031	0.720	0.659
$\nabla^2\rho$ (e/Å^5)	–	–	–
	0.739	–	–
	5.582	2.670	7.561
Δ (Å)	0.08		
	–		
	0.035		
d(B–c.p.) (Å)	0.500	0.942	
	0.505	–	
	0.490	0.940	
d(C-c.p.) (Å)	1.054		
	1.057		
	1.084		

^{a} Values in columns are given in order: Jemmis et al.,[24] Bader and Legar,[23] and this work (experimental data). The ρ_c and $\nabla^2\rho$ are values of the total electron density and its Laplacian in the critical points, respectively (if calculated in refs 23 and 24); Δ is the shift of the bond critical point from the internucelar line; d(B-c.p.) and d(C-c.p.) are distances from the boron and carbon atoms to the (3,−1) bond critical points.

point, i.e. there is a local minimum of $\rho(r)$ at this position. The absolute values of ρ_c in the B–C bonds are very close for both molecules, and they are much larger than corresponding values of the total charge density in the nonbonding B–B regions and centers of the cages. The theoretical value of the Laplacian $\rho(r)$ at the (3,−1) bond critical point of the B–C bond has been calculated only for molecule **I** by Bader and Legare[23] and was found to be slightly positive (Table 3). Our experimental data resulted in the positive Laplacian values for B–B bonds and the center of the cage (that was expected), but also in the high positive Laplacian value in the B–C bond. Probably this result reflects nonsufficient accuracy of the diffraction data. On the other hand, it was noted that the positive Laplacian in the bond critical points is rather characteristic feature of highly polar covalent bonds.[44,45] In accord with calculations[22−24] the B–C bonds in the molecule **I** are very polar, and the same is probably true also for **II**. Some indication for this polarity is a significant shift of the bond critical point position from the center of the B–C bonds to the boron atoms, indicating charge transfer from the boron to axial carbon atoms. This shift is almost the same for B–C bonds in molecules **I** and **II**.

Concluding Remarks

Charge density analysis performed for the single crystal of **II** revealed clearly that the bonding picture in this electron precise molecule is described as a superposition of the conventional localized two-center bonds between B–C and C-C atoms and multicenter bonding in the triangle B–C–B faces of the C_2B_3 cage. The contribution of the nonclassical multicenter bonding to the electronic structure of the molecule has probably the same importance as the conventional two-center one. The localized B–C bonds are essentially bent outward of the cage in the same manner as in the small-ring strained molecules. There was no charge density accumulation found in the B–B–B plane of the molecule, thus indicating the absence of the direct B–B interactions between boron atoms, despite rather short B–B distances. A multipole refinement confirmed main conclusions about the electron density distribution in **II** obtained with a conventional "X−X" method, and corresponding static DED maps reproduced the conventional dynamic ones in all important features. An additional confirmation for the B–C bond bending, the absence of the direct B–B bonds in the central cage and the multicenter bonding in the B–C–B triangle faces has been obtained via the topological analysis of the experimental charge density $\rho(r)$. This analysis revealed also the shift of the (3,−1) bond critical points in the B–C bonds to the boron atoms that is related with the polar nature of these bonds. The main features of the charge density in the electron precise molecule **II** are very close to those for an electron deficient $B_5H_5{}^{2-}$ dianion, where the chemical bonding is described usually in terms of the multicenter bonds. It seems therefore that in small B,C-containing cages, whether a molecule is electron precise or not, the general picture of the bonding represents some superposition of the conventional two-center localized bonding and nonclassical multicenter one.

Supporting Information Available: Tables of the crystal data, experimental conditions and results of the refinement, non-hydrogen atomic coordinates and their anisotropic displacement parameters, bond lengths and bond angles, and H-atom coordinates and their isotropic displacement parameters (4 pages). See any current masthead page for ordering and Internet access instructions.

JA961884I

(44) MacDougall, P. I.; Bader, R. F. W. *Can. J. Chem.* **1986**, *64*,1496−1508.
(45) Bader, R. F. W.; Essen, H. *J. Chem. Phys.* **1984**, *80*, 1943−1960.
(46) After submission this paper we learned about a very recent theoretical calculations by Schleyer et al.[47] of the bonding, energetic, and magnetic properties in the series of five-vertex *closo*-boranes $X_2B_3H_3$ (X = N, CH,P, SiH, BH$^-$) using an *ab initio* (MP2) approximation. The results of these calculations together with the natural bond orbital analysis showed large cage delocalization (nonclassical bonding contribution) in these molecules which is in accord with our finding.
(47) Schleyer, P. v. R.; Subramanian, G.; Dransfeld, A. *J. Am. Chem. Soc.* **1996**, *118*, 9988−9989.